Direct and Chaotic Ionization in the Presence of External Fields: the Transition-State Theory Point of View†

ARTICLE *in* THE JOURNAL OF PHYSICAL CHEMISTRY A · FEBRUARY 2001

Impact Factor: 2.69 · DOI: 10.1021/jp0038761

2 AUTHORS:

Charles Jaffé
West Virginia University
55 PUBLICATIONS **1,193** CITATIONS

SEE PROFILE

T. Uzer
Georgia Institute of Technology
180 PUBLICATIONS **3,185** CITATIONS

SEE PROFILE

Direct and Chaotic Ionization in the Presence of External Fields: the Transition-State Theory Point of View†

Charles Jaffé‡ and T. Uzer*,§

Department of Chemistry, West Virginia University, Morgantown, West Virginia 26506-6049, and School of Physics, Georgia Institute of Technology, Atlanta, Georgia 30332-0430

Received: October 20, 2000; In Final Form: January 23, 2001

The transition state is fundamental to modern theories of reaction dynamics. Although transition-state theory (TST) has been used mainly in chemical physics, it can be applied to any problem that involves some form of transformation, including half-scattering events such as ionization. In this paper, we use TST to investigate the competition between direct and chaotic mechanisms in the ionization of Rydberg atoms in external electric fields.

1. Introduction

"As we read the *Principia* we feel as we are in an ancient armory where the weapons are of a gigantic size; and as we look at them we marvel what manner of man he was who could use them as a weapon what we can scarcely lift as a burden". (Andrade, E. N. da C. *Newton and the Science of his Time*; Royal Society of London: London, U.K., 1943.) These words of the Cambridge scholar William Whewell accurately describe our appreciation for Bill Miller, and we are honored to contribute to this Special Issue in a subject of great interest to him, namely, transition-state theory (TST). Although the use of TST in atomic physics is still a novelty, we hope to show that TST has useful insights to contribute even in areas seemingly remote from its origins.

Recently we exploited the analogy between a unimolecular reaction[1,2] and the ionization of hydrogen in crossed electric and magnetic fields[3,4] to identify, for the first time, a transition state for the process and to compute the ionization rate based on the fractal dynamics.[5,6] We were guided by modern advances in the theory of chemical reaction dynamics[7−13] which recognize that classical phase space structures (bottlenecks, turnstiles, etc.) govern the progress of the reaction.[14,15] Identifying these structures requires techniques from nonlinear dynamics and chaotic scattering theory.[11−13] In this paper, we will apply similar techniques to the ionization of Rydberg atoms with multielectronic cores in an external electric field, a problem which has been gaining in popularity recently.[16−29] In particular, we will show how TST can help us clarify the competition between direct and chaotic ionization in such atoms.

Innovative, sophisticated experimental techniques have recently lead to renewed interest in atoms[30,31] or molecules[32] in which an electron is promoted to a high energy state, where it is only weakly bound to the core and its dynamics are approximately hydrogenic. These states are typically characterized by very large principal quantum numbers ($n \gtrsim 50$),[30] and such atoms (or molecules) are generically said to be in "Rydberg" states, because the energy levels of the excited electron are well described by a Rydberg-like formula.[30]

Rydberg atoms and molecules occupy a special place in the physical sciences, because their loosely bound electron lives in that poorly charted territory where the quantum world of the atom transforms into the classical reality of macroscopic objects. Rydberg atoms have many exaggerated properties such as huge dipole moments, and they constitute very convenient, natural laboratories for the investigation of many physical phenomena which they display with exceptional clarity. Rydberg electrons are very weakly bound, and they reside mostly at an immense distance from the atomic or molecular core, to the point that if the Rydberg atoms were solid, they would be just about visible to the naked eye. Laboratory-scale external fields, and even weak stray electric fields,[33] become comparable to the atomic (or molecular) Coulomb field sensed by the Rydberg electron, and interesting, dynamical properties, such as quantum chaology,[34] can be studied experimentally.

The ionization of a Rydberg atom in external electric fields resembles a chemical reaction: in a typical unimolecular reaction,[1,2] the molecule is first given sufficient energy so that it can overcome the barrier to reaction. Some time after the activation, if energy finds its way into the reactive mode, the reaction occurs. In the problem of the ionization of Rydberg atoms, the "activation" is the initial excitation to a state of very high principal quantum number ($n \sim 50$ or larger). Following state preparation, energy flows into the ionization channel and the electron is detached. In both systems, a central question concerns the rate at which the energy migrates into the reactive (or ionizing) mode. We begin by reviewing TST briefly as it relates to nonlinear dynamics.

The concept of a transition state is central to the theory of chemical reaction dynamics.[35,36] The basic idea, strictly classical in origin, postulates the existence of a minimal set of states that all reactive trajectories must pass through and which is never encountered by any nonreactive trajectories. This set of states is collectively called the "transition state".

The notion of a transition state can be traced to the work of Marcelin[37] in 1915. Subsequently, in 1931, Eyring and Polanyi[38] quantified the idea of a transition state in the collinear $H + H_2$ reaction. Their paper, which can be viewed as the origin of modern theories of chemical reactions, reports the first calculation of the potential-energy surface of a reaction. Immediately following the appearance of this work, Wigner[39] and others[40,41]

† Part of the special issue "William H. Miller Festschrift".
* To whom correspondence should be addressed.
‡ West Virginia University.
§ Georgia Institute of Technology.

10.1021/jp0038761 CCC: $20.00
Published on Web 02/24/2001

developed a variety of very simple, yet extremely useful, theories of bimolecular reactions, for example, activated complex theory and TST . During the following decade, further seminal papers in the development of unimolecular reactions were published.[1,2] Again the concept of a transition state played a central role although these early theories of chemical reactions remained strictly classical in nature. Quantization was the next major step in the development of TST.[42]

Even in the earliest days it was recognized that the transition state as defined by Eyring and Polanyi was in fact not a surface of no return and that trajectories can recross this surface many times[43] because of dynamical effects that can result from cross-terms in the kinetic energy, e.g., dynamical barriers. The recognition of the complex nature of the dynamics led to the development of a variational approach[41,42,44] which considered the set of all possible transition states and then chose the one with the minimum flux across it. The variational problem was solved by demonstrating that the surface of minimum flux, and hence the transition state, must be an unstable periodic orbit whose projection into coordinate space connects the two branches of the relevant equipotentials.[45−48] These surfaces are called periodic orbit dividing surfaces or PODS (as is the convention, the term PODS is both singular and plural[49]). The PODS with the minimum flux is chosen as the transition state.

Although the original idea of a transition state was expressed as a dividing surface in *coordinate* space, it was soon recognized that in a proper treatment dividing surfaces must separate volumes corresponding to reactants and products in *phase space*. Progress in this direction accelerated after advances in dynamical systems theory and computing capability. In the mid 1980s, Davis and co-workers[7−9] showed that the partitioning of phase space can be accomplished using the manifolds[50] of the PODS associated with the transition states. A related approach to the investigation of the structure of phase space of reactive systems, which is closer to our point of view here, is that of Ozorio de Almeida et al.[10] Tiyapan and Jaffé[11−13] extended these ideas considerably and showed that the manifolds of the PODS can be used to construct an invariant fractal tiling of phase space and in the simplest case of complex formation (unimolecular reactions) characterized this fractal structure.

In their study of the Stark ionization of rubidium Rydberg wave packets, Lankhuijzen and Noordam[21,22] observe two distinct mechanisms. They term these "prompt" and "delayed" ionization; we prefer the terms direct and chaotic ionization, by which we mean ionization associated with regular and chaotic classical dynamics, respectively (for further details, see ref 5). In our paper, we use TST to investigate these dynamical mechanisms that lead to the ionization of Rydberg atoms in external electric fields.

Our paper is organized as follows: In the next section, we discuss the one-electron model that we use in our numerical investigation. This model is constructed from hydrogen in an external electric field by adding an effective core potential. After the system is regularized, the Hamiltonian takes a particularly simple form which is readily amenable to analysis. In section 3, we review the role of PODS in the classical theory of transport. In particular, we focus on the definition of the transition state for ionization process in terms of the PODS. The dynamical origins of the two ionization mechanisms are investigated using standard nonlinear dynamical techniques in section 4. Here we see that the chaotic ionization is a direct consequence of the collision of the Rydberg electron with the core of the alkali metal atom. In the last section, we compare results for lithium, sodium, potassium, and rubidium. We observe that the results we obtain for sodium, potassium, and rubidium are qualitatively the same. Our results for lithium are remarkably different; the explanation of these differences must await a more detailed investigation.

2. Stark Effect in Alkali Metals

A discussion of classical field ionization of the alkali metals should begin by reviewing the electron dynamics in a hydrogen atom.[51] The addition of an electric field, which gives rise to the Stark effect, leads to the onset of direct ionization of the hydrogen. Chaotic ionization is observed with the addition of the core potential. Our approach of starting with the classical potential of a hydrogen atom and then adding the electric field and core potential as perturbations provides a clear picture of the origin of both the direct and chaotic ionization.

2.1. Classical Dynamics of the Hydrogen Atom. The classical Hamiltonian for a hydrogen atom (in atomic units) is given by

$$H = \frac{1}{2}(p_x^2 + p_y^2 + p_z^2) - \frac{1}{r} \tag{1}$$

where $r = (x^2 + y^2 + z^2)^{1/2}$. This system has three degrees of freedom, and thus, the dynamics are confined to a six-dimensional phase space. In the traditional treatment of the dynamics, the three independent constants of the motion can be taken as the total energy, the total angular momentum, and the projection of the angular momentum on a space-fixed axis. A classical trajectory is confined to a three-dimensional subspace within the six-dimensional phase space. The topology of this subspace is a three-dimensional torus, and the subspace is often called an invariant torus. Additional symmetries, usually referred to as the hidden symmetries, exist and are related to the Runge-Lenz vector.[52] The existence of these hidden symmetries is revealed by the existence of additional constants of the motion which, in turn, further restrict the dynamics. These additional constraints conspire to make all classical trajectories periodic orbits, that is, confined to one-dimensional subspaces on the invariant tori.

In the traditional study of the electron dynamics in hydrogen, one separates the variables to reduce the problem from three degrees of freedom to three one-degree-of-freedom problems. As a consequence of hidden symmetries, the hydrogen atom can be separated in several different sets of variables. The choice of which set of variables to use depends on the application. In the present study, the semiparabolic variables are the most convenient.

In the hydrogen atom, the electron is bound to the nucleus for all negative energies. The classical trajectories (which are periodic orbits) lie in a plane and are ellipses. The geometrical properties of the periodic orbits depend on the values of the constants of the motion. The size of the orbits depends on the principal action (which corresponds to the principal quantum number), the plane of the orbit is determined by the projection of the total angular momentum on a space-fixed axis, the orientation of the ellipse within the plane depends on the Runge−Lenz vector, and the eccentricity of the ellipse depends on the total angular momentum. The periodic orbit becomes a circle as the angular momentum approaches its maximum value. As the angular momentum approaches zero, the periodic orbit reduces to a straight line passing through the nucleus.

2.2. Stark Effect in the Hydrogen Atom. Placing a hydrogen atom in an electric field has important consequences for the dynamics of the electron. For the purposes of the present discussion, the most important of these is that the ionization

threshold is lowered. In other words, if a highly excited but bound hydrogen atom is placed in an electric field, it may ionize.

The classical Hamiltonian for a hydrogen atom in a static electric field is given by (in atomic units)

$$H = \frac{1}{2}(p_x^2 + p_y^2 + p_z^2) - \frac{1}{r} - Ez \tag{2}$$

where the z axis is chosen in the direction of the electric field and E is the strength of the electric field in atomic units of $E_0 = e^5 m_e^2/\hbar^4 = 5.14 \times 10^{11}$ V/m. The introduction of the electric field destroys some of the constants of the motion. Three independent constants of the motion remain (and no additional hidden symmetries), and the dynamics are confined to three-dimensional invariant tori. We take the total energy to be the first constant of the motion. To identify the other two constants of the motion, we will first transform the Hamiltonian from Cartesian into cylindrical coordinates and then into semiparabolic coordinates.[51] This canonical transformation is given by

$$\begin{aligned} x &= \rho\cos\varphi \qquad p_x = p_\rho\cos\varphi - \frac{p_\varphi}{\rho}\sin\varphi \\ y &= \rho\sin\varphi \qquad p_y = p_\rho\sin\varphi + \frac{p_\varphi}{\rho}\cos\varphi \\ z &= z' \qquad p_z = p_{z'} \end{aligned} \tag{3}$$

The transformed Hamiltonian is

$$H = \frac{1}{2}\left(p_\rho^2 + \frac{p_\varphi^2}{\rho^2} + p_z^2\right) - \frac{1}{r} - Ez \tag{4}$$

where $r = (\rho^2 + z^2)^{1/2}$ and where we have dropped the primes. The Hamiltonian does not depend on the angle φ (which is an ignorable coordinate), and thus p_φ is a constant of the motion, namely, the projection of the total angular momentum on the z axis defined by the electric field; we will label it l_z.

Next we transform from cylindrical into semiparabolic coordinates. The canonical transformation to semiparabolic coordinates is given by

$$\begin{aligned} \rho &= u\upsilon \qquad p_\rho = \frac{\upsilon p_u + u p_\upsilon}{u^2 + \upsilon^2} \\ z &= \frac{1}{2}(u^2 - \upsilon^2) \qquad p_z = \frac{u p_u - \upsilon p_\upsilon}{u^2 + \upsilon^2} \\ \varphi &= \varphi' \qquad p_\varphi = p_{\varphi'} \end{aligned} \tag{5}$$

and the transformed Hamiltonian is

$$H = \frac{1}{2}\left(\frac{p_u^2 + p_\upsilon^2}{u^2 + \upsilon^2} + \frac{l_z^2}{u^2\upsilon^2}\right) - \frac{2}{u^2 + \upsilon^2} - \frac{E}{2}(u^2 - \upsilon^2) \tag{6}$$

Next we define a new Hamiltonian; we do this by multiplying both side of eq 6 by $(u^2 + \upsilon^2)$ and then rearranging the terms.[53] This yields

$$K = 2 = \frac{1}{2}\left(p_u^2 + p_\upsilon^2 + \frac{l_z^2}{u^2} + \frac{l_z^2}{\upsilon^2}\right) + \frac{\omega^2}{2}(u^2 + \upsilon^2) - \frac{E}{2}(u^4 - \upsilon^4) \tag{7}$$

where we have defined $\omega = (-2H)^{1/2}$. Observe that the new Hamiltonian is *not* equal to the energy but rather is a constant,

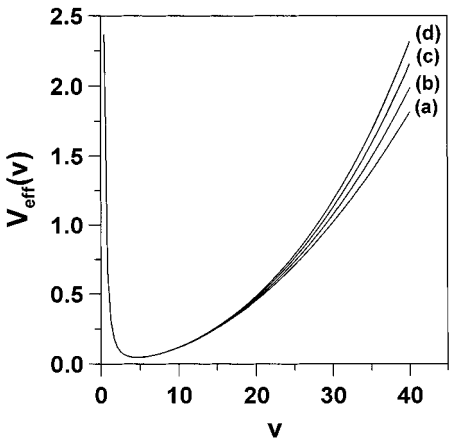

Figure 1. Potential energy in the υ degree of freedom for hydrogen in an electric field. The four curves correspond to different electric field strengths in atomic units: (a) $E = 0.0$, (b) $E = 1.327 \times 10^{-7}$, (c) $E = 2.645 \times 10^{-7}$, (d) $E = 3.891 \times 10^{-7}$.

i.e., $K = 2$. The variable conjugate to the new Hamiltonian, which is a time-like variable, is defined by[53]

$$\frac{d\tau}{dt} = (u^2 + \upsilon^2)^{-1} \tag{8}$$

We can separate the new Hamiltonian into two parts, each depending on one of the variables and its conjugate momentum:

$$K = 2 = \frac{1}{2}\left(p_u^2 + \frac{l_z^2}{u^2} + \omega^2 u^2 - Eu^4\right) + \frac{1}{2}\left(p_\upsilon^2 + \frac{l_z^2}{\upsilon^2} + \omega^2\upsilon^2 + E\upsilon^4\right) \tag{9}$$

The resulting two constants of the motion are, however, not independent because the new Hamiltonian is a constant. We define the third dependent constant of motion as

$$K_u = \frac{1}{2}\left(p_u^2 + \frac{l_z^2}{u^2} + \omega^2 u^2 - Eu^4\right) \tag{10}$$

In the zero-field limit, the Hamiltonian of eq 9 reduces to the sum of two identical harmonic oscillators with a centrifugal barrier at the origin. The harmonic frequency is proportional to the square root of the total energy (this reduction is only valid for negative energies). The electric field introduces quartic terms with opposite signs into both harmonic oscillators. In the υ degree of freedom, the quartic term is positive. As the electric field is increased, the outer wall becomes steeper (see Figure 1), and this in turn increases the frequency of the oscillator. On the other hand, because of the negative sign of the quartic term for the u degree of freedom, the potential is always negative for large u, and it is in this degree of freedom that the system can ionize (Figure 2). The height of the barrier to ionization decreases as the strength of the electric field increases. If the height of the barrier is greater than 2, then ionization is classically forbidden. Although the requirement that the barrier height be less than 2 is a necessary condition for ionization, it is not sufficient. In addition, we must also require that the third constant of the motion be greater than the barrier height. In these circumstances, the system will exhibit direct ionization. Contour plots of the two-dimensional effective potential are shown in Figure 3a for semiparabolic coordinates and in Figure 3b for polar coordinates.

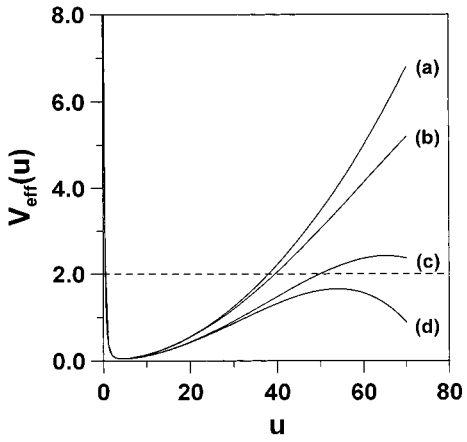

Figure 2. Potential energy in the *u* degree of freedom (ionization mode) for hydrogen in an electric field. The four curves correspond to different electric field strengths in atomic units: (a) $E = 0.0$, (b) $E = 1.327 \times 10^{-7}$, (c) $E = 2.645 \times 10^{-7}$, (d) $E = 3.891 \times 10^{-7}$. The dashed line is the ionization threshold.

TABLE 1: Parameters for the Effective Potential Modeling of the Cores of Lithium, Sodium, Potassium, and Rubidium[a]

	Z	α_1	α_2	α_3		Z	α_1	α_2	α_3
Li	3	3.310	3.310	3.310	K	19	3.474	10.590	1.725
Na	11	7.902	23.510	2.688	Rb	37	3.41	10.098	1.611

[a] See ref 54 and eq 11.

2.3. Stark Effect in Alkali Metal Atoms. The introduction of an effective potential to model the influence of the core electrons has a significant impact on the dynamics of the outer electron. In particular, a chaotic component is introduced into the ionization. The classical Hamiltonian for an alkali metal atom in a static electric field is given by (in atomic units)

$$H = \frac{1}{2}(p_x^2 + p_y^2 + p_z^2) - \frac{1 + W(r)}{r} - Ez \qquad (11)$$

where

$$W(r) = (Z - 1)e^{-\alpha_1 r} + \alpha_2 r e^{-\alpha_3 r} \qquad (12)$$

where the constants are given in Table 1.[54] Here Z is the nuclear charge and the α's are optimized numerically so as to reproduce the field free energy levels and, hence, the quantum defects of the for the alkali metal atoms.

Using the same procedure as discussed above for hydrogen we obtain the following new Hamiltonian (in semiparabolic coordinates) for an alkali metal atom in an electric field:

$$K = 2 = \frac{1}{2}\left(p_u^2 + \frac{l_z^2}{u^2} + \omega^2 u^2 - Eu^4\right) + \frac{1}{2}\left(p_v^2 + \frac{l_z^2}{v^2} + \omega^2 v^2 + Ev^4\right) - W(r) \quad (13)$$

where $r = {}^1/_2(u^2 + v^2)$. The effect of the core potential is to couple the two quartic oscillators.

It is instructive to compare the effective potentials of hydrogen and potassium. With the exception of the immediate vicinity of the core, these two potentials are identical. Expansion of the core region of the potentials for hydrogen and potassium are shown in semiparabolic coordinates in Figure 4 and in polar coordinates in Figure 5. Clearly, the morphology of the potential-energy surface is changed by the addition of the core potential.

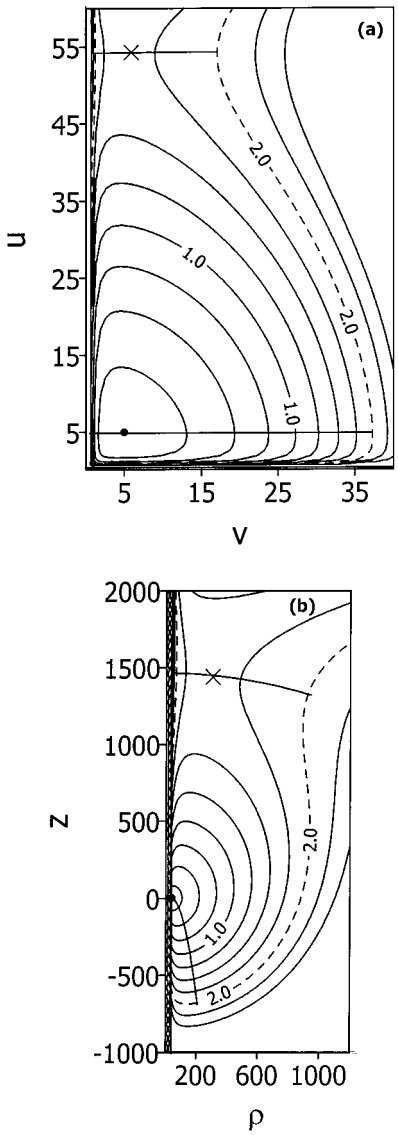

Figure 3. Potential-energy surface for hydrogen ($\omega = {}^1/_{21} \simeq 0.047\,619\,0$, $l_z = 1$) in two different coordinate systems (a) semiparabolic and (b) cylindrical. The two PODS that occur for hydrogen are also shown. The PODS corresponding to the ionization transition state passes through the cross, which shows the position of the saddle point. The second PODS, which we use to construct our surfaces of sections, passes through the solid circle that shows the position of the minimum of the Coulomb well.

The potential-energy surface for hydrogen has a single minimum and a single saddle point. The minimum corresponds to the bottom of the Coulombic well, and the saddle point sits on the barrier between the bound and ionized regions. This is clearly seen in Figure 3. The introduction of the core potential results in an additional minimum and saddle. The minimum lies interior to the core, and the saddle point lies on a barrier that separates the core well from the Coulombic well. These can be clearly seen in Figures 4b and 5b. The other alkali metal potentials have the same morphology as seen here for potassium; the differences are the depth and position of the core well and the height and position of the barrier separating the core well from the Coulombic well.

In summary, the potential that we use to model the ionization of alkali metal atoms in an electric field is constructed by adding a core potential and an electric field to the potential of hydrogen. The core terms only affect the potential in the immediate region of the core. The electric field has minimal influence in this

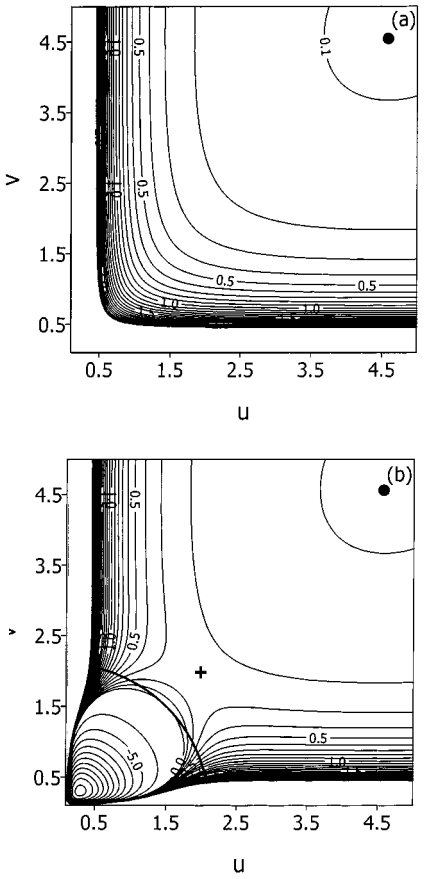

Figure 4. Expansion of the potential-energy surfaces of (a) hydrogen and (b) potassium at the core of the atom in semiparabolic coordinates. Comparing these two figures reveals the differences between the potential of hydrogen and those of the alkali metals. The well due to the effective core potential is clearly revealed in b. Also seen in this figure is the PODS corresponding to the transition state separating the core well from the Coulomb well. The cross in this figure shows the location of the saddle point between the two wells.

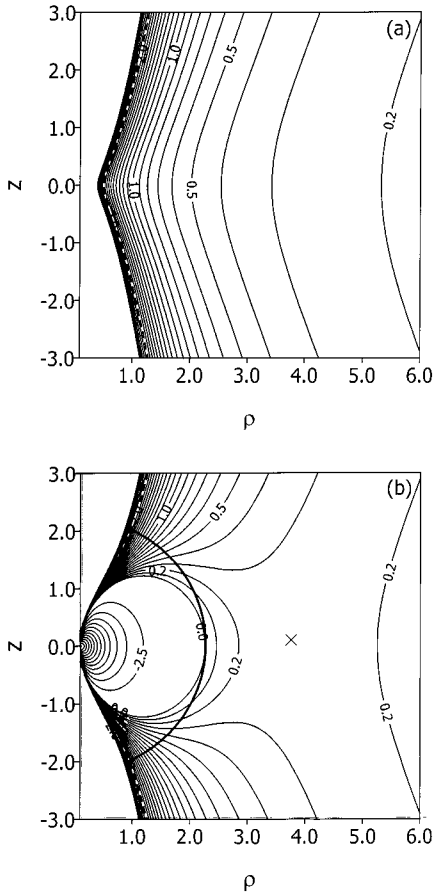

Figure 5. Same as Figure 4 except in cylindrical coordinates.

region. On the other hand, the electric field has significant impact at a large radius, opening up a channel for ionization. In this regime, the core potential has negligible impact.

3. Transport in Hamiltonian Systems

In chemistry, one wishes to determine the rate at which a system passes from one region of configuration space, characterized by reactant configurations, to another, characterized by product configurations. The standard approach is to define a surface that partitions the configuration space into two distinct regions, the first associated with reactants and the second with the products. Once this transition state is defined, the transport problem can be formulated in terms of the directional flux across the surface. The actual definition of this surface matters greatly. Consider the evolution of the system as characterized by a particular trajectory. Clearly, if this trajectory crosses the transition state more than once, then it will contribute to the flux more than once. This will lead to an overestimation of the directional flux (known as the "recrossing" problem). Ideally, one wishes to define the transition state such that it is a surface of no return, that is, such that no trajectory crosses it more than once, a particularly difficult task in diffusion phenomena.[55]

It was in an effort to minimize the recrossing problem that the variational definition of the transition state was formulated. In this formulation, one considers all possible transition states, that is, all surfaces in configuration space which partition the space into two regions. The transition state is then chosen as the surface with minimum directional flow across it. As mentioned previously, for systems with two degrees of freedom, the transition state is the projection of a periodic orbit into the configuration space.[48] In order for this projection to partition the coordinate space, it must touch the classical boundaries of the configuration space at two different points. In general, there is more than one of these surfaces, which Pechukas named PODS. The PODS with the minimum directional flux is chosen as the transition state. The solution of the variational problem for more than two degrees of freedom remains an open question.

Although the rate problem is defined in terms of transport between two different regions of configuration space, the correct formulation of the flow must be in phase space. This immediately raises the question of what role the PODS play in phase space. Their role depends on their stability: The dynamics in the immediate vicinity of a stable PODS will be confined to invariant tori and, as a consequence, will cross the transition state an infinite number of times. In other words, the PODS forms an elliptical center of order. Clearly, a stable PODS cannot be the transition state. On the other hand, an unstable PODS possesses stable and unstable manifolds which partition the energy shell. Consider, for example, the stable manifold. All of the trajectories interior to this manifold will cross the PODS, whereas those exterior to the manifold will not cross the PODS. Thus, the flow in phase space bifurcates into two streams when it encounters the hyperbolic centers characteristic of unstable PODS. In general, the transition state corresponds to the unstable (hyperbolic) PODS with the minimum directional flux.

The presence of more than a one PODS in a dynamical system has important consequences for the transport properties. These are most clearly illustrated by considering the well-studied

collinear atom−diatom reaction $H + H_2$.[9,36] In this example, a potential barrier separates the reaction and product valleys. For low-energy collisions, this system has a single PODS that sits on top of the potential barrier. It is unstable and corresponds to the transition state. As the collision energy is increased, additional PODS appear at saddle-center bifurcations.[50] At such bifurcations, two new PODS are born out of nothing, one stable and the other unstable. Because of the symmetry of the system, the two saddle-center bifurcations occur at the same energy on either side of the original PODS. Immediately above this energy there are five PODS. Three of which are unstable, and two which are stable. The sequence along the reaction coordinate is unstable, stable, unstable, stable, and unstable. The two outer unstable PODS sit on top of dynamical (as opposed to potential) barriers. The two stable PODS correspond to the periodic motion that is trapped between the outer dynamical barrier and the central potential barrier. In other words, the system is trapped in an effective well. In the simplest theories of chemical reactions, one would take the last of the PODS, that is, the one furthest out in the product channel, as the transition state. However, more realistic theories will recognize that the three unstable PODS partition configuration space into four separate regions, and that the rate problem will involve the transport between these four regions.

In the second section, we introduced the Hamiltonian systems that we use to model the Stark ionization of alkali metals. The identification and characterization of the PODS for these systems is simple and straightforward. To find the PODS we consider the set of trajectories which initially are confined to the $K = 2$ equipotential as obtained from eq 13. We propagate these trajectories forward in time and determine their next intersection with the Poincaré surface of section defined by $p_v = 0$ and $\dot{p}_v \geq 0$.[56] This surface of section is particularly useful because the line defined by $p_u = 0$ is the equipotential. Thus, trajectories that intersect this surface of section with $p_u = 0$ intersect both branches of the equipotentials and therefore correspond to PODS.

For the pure Coulomb case (hydrogen), there are two PODS. These are shown in Figure 3. The first sits on top of the barrier to ionization and corresponds to the ionization transition state. It is unstable. The second PODS is stable and sits at the bottom of the Coulombic well. In the next section, we will use this PODS to construct surfaces of section.

With the introduction of the core potential, two additional PODS make their appearance. The first of these is unstable and sits on top of the barrier between the Coulombic and the core wells. This PODS is shown in Figures 4b and 5b. The last PODS is initially stable and sits in the core well. It is important to observe that the two PODS associated with the pure coulomb case occur in the region of coordinate space that is unaffected by the core potential and thus are virtually identical for hydrogen and the alkali metals. (With great care, numerical differences can be observed between the stable PODS. However, these differences are so minimal that no consequences are observed. We were unable to observe analogous differences in the unstable PODS.) In the next section, we will use these PODS to investigate the phase space flow and to illustrate the origin of the chaotic ionization in the Stark ionization of the alkali metals. Details of the operational aspects of our calculation can be found in our publication on the transition state in atomic physics.[5]

4. Chaotic vs Direct Ionization

The field ionization of hydrogen proceeds by a direct mechanism: once the system has been excited with enough energy in the ionization mode, it ionizes immediately. On the other hand, the field ionization of the alkali metals can proceed by either of two mechanisms: a direct mechanism analogous to that of hydrogen and an indirect or chaotic mechanism. In this section, we will present the results of our numerical study of the classical transport involved in ionization alkali metals which clearly illustrates the origin of the second mechanism. The basic difference between these two mechanisms lies in the redistribution of the internal energy. In the direct mechanism, the system is excited in such a manner that there is sufficient energy in the ionization channel and ionization can occur without redistribution of the excitation, as a result the system ionizes immediately. On the other hand, the chaotic mechanism requires the redistribution of the energy. That is, following the initial excitation, the energy is not in a mode that will led to ionization. In order for ionization to occur, the energy must be redistributed. This can only happen through a collision of the electron with the core.

It is also useful to make the comparison between direct and chaotic ionization in the half-scattering problem and direct and chaotic scattering in the full-scattering problem. In the full-scattering problem, trajectories corresponding to direct scattering events are characterized by a single inner turning point, whereas trajectories corresponding to chaotic scattering will have many inner turning points. In other words, for direct scattering dynamics, a full set of local constants of the motion (i.e., one for each degree of freedom) can be defined, and thus, redistribution of energy between the modes will not occur. For chaotic scattering events, a full set of local constants of the motion cannot be defined, and redistribution of the energy will occur. As a consequence, complexes are formed. In the half-scattering problem, the situation is the same. The dynamics associated with direct ionization is characterized by the existence of a full set of local constants of the motion, whereas the dynamics associated with chaotic ionization do not possess a full set of local constants of the motion. The difference between these two phenomena lies in the initial conditions. For the full-scattering problem, the system is initialized prior to the collision, whereas in the half-scattering problem, the system is initialized in the middle of the collision. Thus, chaotic (direct) ionization in the half-scattering problem corresponds to chaotic (direct) scattering in the full-scattering problem.

Our approach to investigating the ionization mechanism is to first identify the configurations that will ionize within the next period.[5] We define the period in terms of the original physical variables. We have chosen to investigate the dynamics for a single energy ($H = -1/882 \simeq -0.001\,133\,786\,8$, $\omega = 1/21 \simeq 0.047\,619\,0$) for $l_z = 1$ and for an electric field of $E = 3.891 \times 10^{-7}$ atomic units. Once we have identified these configurations, we will investigate their prior dynamical history. To identify the configurations that will ionize within the next period we consider the surface of section defined by the stable PODS lying at the bottom of the Coulomb well (the curve near $u = 5$ in Figure 3a). All classical trajectories that cross the ionization transition state must cross this PODS immediately prior to crossing of the transition state. By "immediately prior", we mean that the classical trajectory will not encounter any classical turning points in the period of time between the crossing of the two PODS. To identify these configurations we follow the stable manifold backward in time until it crosses the surface of section PODS. The intersection of the surface of section and the stable manifold will be a closed curve which is shown in Figure 6. The outer closed curve seen in this figure is the classical boundary of the surface of section. All classically allowed

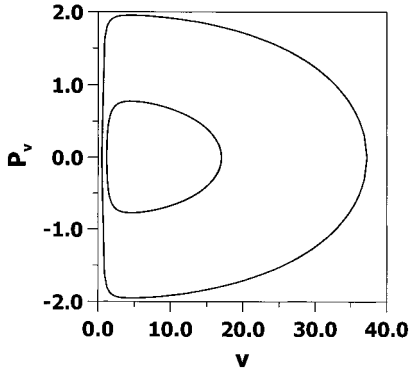

Figure 6. Surface of section for potassium. The outer curve is the boundary of the classically allowed region. The inner curve is the last intersection of the stable manifold of the PODS corresponding to the ionization transition state. The area interior to the inner curve represents the configuration that will ionize within the next period.

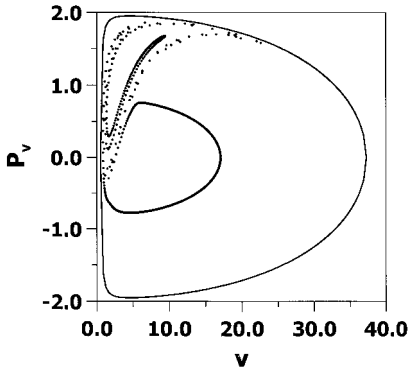

Figure 7. Surface of section for potassium. The outer curve is the boundary of the classically allowed region. The inner curve is the first intersection of the unstable manifold of the PODS corresponding to the ionization transition state. The area interior to inner curve represent the configurations that have been captured by the potassium ion in the previous period.

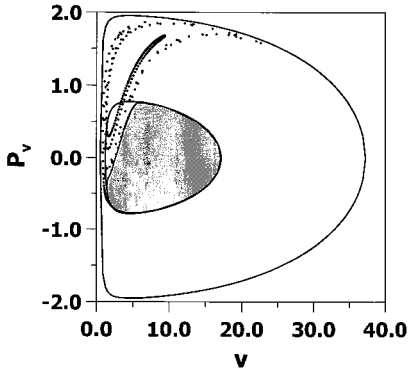

Figure 8. Surface of section for potassium. We show the first intersection of the unstable manifold and the last intersection of the stable manifold of the ionization PODS. The shaded area is interior to both of these intersections and corresponds to the configurations that ionize via the direct mechanism.

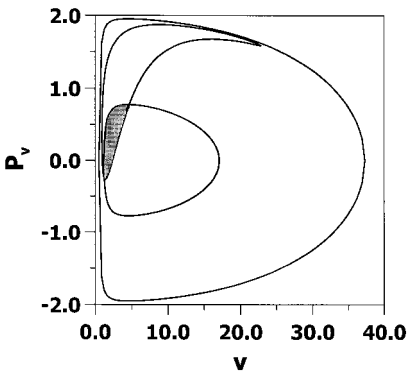

Figure 9. Surface of section for potassium. We show the first intersection of the unstable manifold of the PODS separating the core well from the Coulomb well superimposed with the last intersection of the stable manifold of the ionization PODS. The shaded area corresponds to the configurations which ionize immediately following a collision with the core, that is, via the chaotic mechanism.

configurations must lie within this curve. The inner closed curve is the last intersection of the stable manifold of the PODS corresponding to the ionization transition state with the surface of section. All of the configurations lying within this curve will ionize within the next period. The property of being within this curve is both a necessary and sufficient condition for immediate ionization. The vast majority of the configurations within the classically allowed region of the surface of section will eventually ionize. It is only those within the inner curve that will ionize immediately. We now investigate the dynamical histories of the configurations that lie within this closed curve.

The configurations within the inner closed curve in Figure 6 ionize within the next period. To identify the configurations which correspond to direct ionization, we consider the unstable manifold of the transition state PODS. The first intersection of this manifold with the surface of section is shown in Figure 7. The configurations that lie within this curve were captured by the ionic core within the previous period. Also shown here is the classical boundary of the surface of section.

The configurations that correspond direct ionization are those that lie within both the first intersection of the unstable manifold of the transition state PODS and the last intersection of the stable manifold of the transition state PODS. These two intersections are superimposed in Figure 8. The configurations in the shaded region correspond to direct ionization. The trajectories also correspond to direct scattering. They encounter a single inner turning point and no outer turning points.

It remains to identify the dynamical character of the configurations that ionize within the next period but whose mechanism of ionization is not direct. To characterize these configurations, consider the PODS that lies on top of the barrier between the core well and the Coulomb well. Follow the unstable manifold of this PODS forward in time until it intersects the surface of section. This yields a closed curve. The configurations interior to this curve correspond to configurations that have just escaped from the core well, that is, that have just suffered a collision with the core. This curve is shown in Figure 9 together with the curve obtained from the last intersection of the stable manifold of the transition state PODS. The region interior to both of these curves (shaded) is the configurations that ionize immediately following a collision with the core.

The dynamical origins of the configurations that will ionize within the next period are shown in Figure 10. The outer curve in this figure is the last intersection of the stable manifold of the transition state PODS with our surface of section. Of the two shaded areas, the one labeled D corresponds to configurations which ionize via the direct mechanism and the other (labeled C) corresponds to configurations that ionize via chaotic mechanism following a collision with the core. The region separating these two shaded areas will also ionize via a chaotic mechanism. Many details of the dynamical histories of these configurations remain to be investigated. We have observed that many of these configurations do suffer from a collision with the core prior to ionization; however, the ionization does not

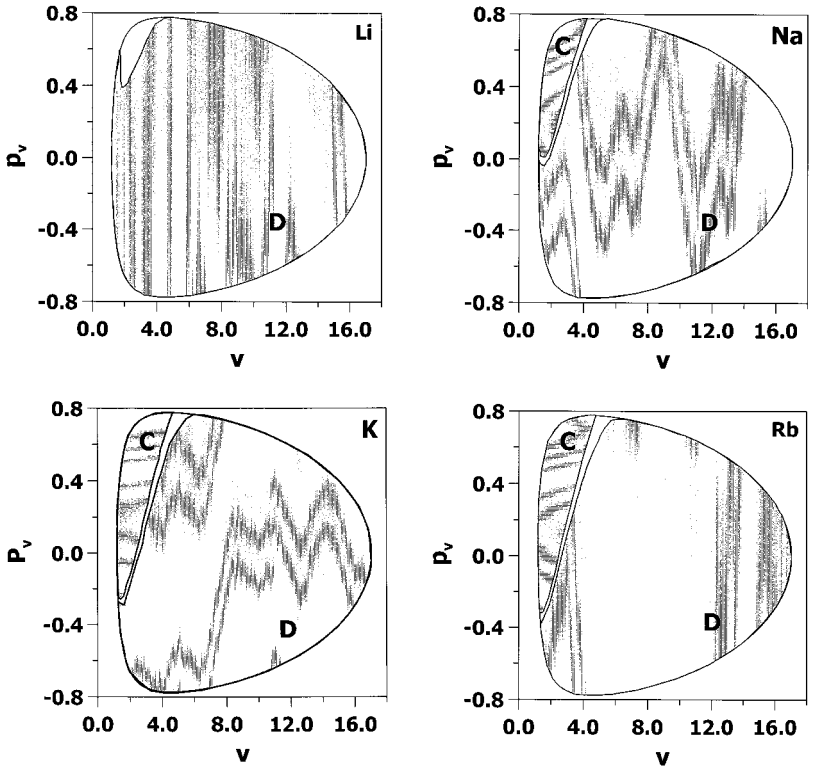

Figure 10. Here we compare the results for the different alkali metal atoms lithium, sodium, potassium, and rubidium that we investigated. The shaded areas labeled D correspond to configurations that ionize via the direct mechanism, whereas the shaded areas labeled C correspond to configurations that ionize via the chaotic mechanism immediately following a collision with the core. Note that although the results for sodium, potassium, and rubidium are qualitatively the same, the results for lithium are very different. For lithium, the PODS separating the core well from the Coulomb well apparently does not exist.

occur immediately following the collision but rather after one or more periods following the collisions with the core.

5. Discussion

We have investigated the two dynamical mechanisms that lead to the ionization of Rydberg electrons in highly excited alkali metal atoms. The first of these is the direct mechanism where the atomic system is excited in such a manner that the Rydberg electron has sufficient energy in the ionization mode and can ionize immediately. In the full scattering problem, it corresponds to direct scattering.

The second mechanism requires collisions with the core. Here the atomic system is excited in such a manner that the Rydberg electron does not have sufficient energy in the ionization mode, and the energy of the system must be redistributed for ionization to occur which then takes place through collisions with the core. In examining Figure 9, it is clear that only a small portion of the collisions leads to a effective redistribution of the energy, that is, the majority of the collisions result in a redistribution of the energy that does not lead to ionization. These configurations will eventually ionize, but the vast majority of them will require at least another collision with the core. To this point we have presented results for potassium, although we have also examined the dynamics for lithium, sodium, and rubidium. These results are shown in Figure 10. The results for sodium and rubidium are qualitatively similar to the potassium results, the sole difference being the relative proportion of the configuration that ionize via the chaotic versus the direct mechanism. Reasonably, deeper core wells support more of the chaotic mechanism. It is remarkable that, although lithium also has a core well, it does not appear to support a PODS (transition state) separating it from the Coulomb well. In other words, the Rydberg electron cannot be trapped within the core well. This is very different from the behavior observed in the other three alkali metals that we investigated. To unravel and understand this behavior will require additional numerical investigations, which are currently underway, and will be reported in a future publication.

Acknowledgment. We thank the National Science Foundation for its support of this research.

References and Notes

(1) Forst, W. *The Theory of Unimolecular Reactions*; Academic: New York, 1973.
(2) Robinson, P. J.; Holbrook, K. A. *Unimolecular Reactions*; Wiley: New York, 1992.
(3) Uzer, T.; Farrelly, D. *Phys. Rev. A* **1995**, *52*, R2501.
(4) Milczewski, von J.; Farrelly, D.; Uzer, T. *Phys. Rev. A* **1997**, *56*, 657.
(5) Jaffé, C.; Farrelly, D.; Uzer, T. *Phys. Rev. A* **1999**, *60*, 3833.
(6) Jaffé, C.; Farrelly, D.; Uzer, T. *Phys. Rev. Lett.* **2000**, *84*, 610.
(7) Davis, M. J.; Gray, S. K. *J. Chem. Phys.* **1986**, *84*, 5389.
(8) Davis, M. J. *J. Chem. Phys.* **1987**, *86*, 3978.
(9) Davis, M. J. *J. Phys. Chem.* **1988**, *92*, 3124.
(10) Ozorio de Almeida, A. M.; de Leon, N.; Mehta, M. A.; Marston, C. C. *Physica D* **1990**, *46*, 265.
(11) Tiyapan, A.; Jaffé, C. *J. Chem. Phys.* **1993**, *99*, 2765.
(12) Tiyapan, A.; Jaffé, C. *J. Chem. Phys.* **1994**, *101*, 10393.
(13) Tiyapan, A.; Jaffé, C. *J. Chem. Phys.* **1995**, *103*, 5499.
(14) Wiggins, S. *Chaotic Transport in Dynamical Systems*; Springer-Verlag: New York, 1992.
(15) Wiggins, S. *Normally Hyperbolic Invariant Manifolds in Dynamical Systems*; Springer-Verlag: New York, 1994.
(16) Gao, J.; Delos, J. B. *Phys. Rev. A* **1994**, *49*, 869.
(17) Kondratovich, V.; Delos, J. B. *Phys. Rev. A* **1997**, *56*, R5.
(18) Spellmeyer, N.; Kleppner, D.; Haggerty, M. R.; Kondratovich, V.; Delos, J. B.; Gao, J. *Phys. Rev. Lett.* **1997**, *79*, 1650.
(19) Beims, M. W.; Kondratovich, V.; Delos, J. B. *Phys. Rev. Lett.* **1998**, *81*, 4537.

(20) Dando, P. A.; Monteiro, T. S.; Delande, D.; Taylor, K. T. *Phys. Rev. A* **1996**, *54*, 127.
(21) Lankhuijzen, G. M.; Noordam, L. D. *Phys. Rev. A* **1995**, *52*, 2016.
(22) Lankhuijzen, G. M.; Noordam, L. D. *Phys. Rev. Lett.* **1996**, *76*, 1784.
(23) Lankhuijzen, G. M.; Robicheaux, F.; Noordam, L. D. *Phys. Rev. Lett.* **1997**, *79*, 2427.
(24) Rabani, E.; Levine, R. D.; Mühlpfordt, A.; Even, U. *J. Chem. Phys.* **1995**, *102*, 1619.
(25) Bellomo, P.; Farrelly, D.; Uzer, T. *J. Chem. Phys.* **1997**, *107*, 2499.
(26) Bellomo, P.; Farrelly, D.; Uzer, T. *J. Chem. Phys.* **1998**, *108*, 5295.
(27) Courtney, M.; Jiao, H.; Spellmeyer, N.; Kleppner, D. *Phys. Rev. Lett.* **1994**, *73*, 1340.
(28) Courtney, M.; Jiao, H.; Spellmeyer, N.; Kleppner, D. *Phys. Rev. A* **1995**, *51*, 3604.
(29) Courtney, M.; Kleppner, D. *Phys. Rev. A* **1996**, *53*, 178.
(30) Gallagher, T. F. *Rydberg Atoms*; Cambridge University Press: Cambridge, U.K., 1994.
(31) Connerade, J.-P. *Highly Excited Atoms*; Cambridge University Press: Cambridge, U.K., 1998.
(32) Herzberg, G. *Annu. Rev. Phys. Chem.* **1987**, *38*, 27.
(33) Bellomo, P.; Farrelly, D.; Uzer, T. *J. Phys. Chem. A* **1997**, *101*, 8902.
(34) Gutzwiller, M. C. *Chaos in Classical and Quantum Mechanics*; Springer-Verlag: New York, 1990.
(35) Eyring, H.; Walter, J.; Kimball, G. E. *Quantum Chemistry*; Wiley: New York, 1944.
(36) Pollak, E. In *Theory of Chemical Reaction Dynamics*; Baer, M., Ed.; CRC Press: Boca Raton, FL, 1985; Vol. III, p 123.
(37) Marcelin, A. *Ann. Chim. Phys.* **1915**, *3*, 158.
(38) Eyring, H.; Polanyi, M. *Z. Physik. Chem. B* **1931**, *12*, 279.
(39) Wigner, E. P. *J. Chem. Phys.* **1937**, *5*, 720.
(40) Evans, M. G.; Polanyi, M. *Trans. Faraday. Soc.* **1935**, *31*, 875.
(41) Horiuti, J. *Bull. Chem. Soc. Jpn.* **1937**, *13*, 210.
(42) Keck, J. C. *Adv. Chem. Phys.* **1967**, *13*, 85.
(43) Hirschfelder, J. O.; Wigner, E. *J. Chem. Phys.* **1939**, *7*, 616.
(44) Koeppl, G. W. *J. Am. Chem. Soc.* **1974**, *96*, 6539.
(45) Pechukas, P.; McLafferty, F. J. *J. Chem. Phys.* **1973**, *58*, 1622.
(46) Pechukas, P.; Pollak, E. *J. Chem. Phys.* **1979**, *71*, 2062.
(47) Pollak, E.; Pechukas, P. *J. Chem. Phys.* **1978**, *69*, 1218.
(48) Pechukas, P. In *Dynamics of Molecular Collisions, Part B*; Miller, W. H., Ed.; Plenum Press: New York, 1976; p 269.
(49) Pechukas, P. *Annu. Rev. Phys. Chem.* **1981**, *32*, 159.
(50) Lichtenberg, A. J.; Lieberman, M. A. *Regular and Chaotic Dynamics*; Springer: New York, 1992.
(51) Born, M. *The Mechanics of the Atom*; G. Bell: London, 1927.
(52) Goldstein, H. *Classical Mechanics*; Addison-Wesley: Reading, MA, 1980.
(53) Stiefel, E. L.; Scheifele, G. *Linear and Regular Celestial Mechanics*; Springer-Verlag: Berlin, 1971.
(54) Dando, P. A.; Monteiro, T. S.; Jans, W.; Schweizer, W. *Prog. Theor. Phys. Suppl.* **1994**, *116*, 403.
(55) Toller, M.; Jacucci, G.; DeLorenzi, G.; Flynn, C. P. *Phys. Rev. B* **1985**, *32*, 2082.
(56) The surface of section defined here is not the standard surface of section that chemists have traditionally used. To see that it is in fact equivalent to the usual definition, recall that in the Hamiltonian formulation of classical mechanics the identity of the momenta and coordinates can be interchanged by a simple canonical transformation (see ref 52).